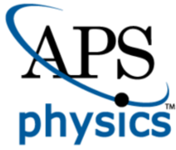

CHORUS

This is the accepted manuscript made available via CHORUS. The article has been published as:

Exploring the energy landscape of resistive switching in antiferromagnetic Sr_{3}Ir_{2}O_{7}

Morgan Williamson, Shida Shen, Gang Cao, Jianshi Zhou, John B. Goodenough, and Maxim Tsoi

Phys. Rev. B **97**, 134431 — Published 27 April 2018

DOI: 10.1103/PhysRevB.97.134431

Exploring the energy landscape of resistive switching in antiferromagnetic $Sr_3Ir_2O_7$

Morgan Williamson[1,2], Shida Shen[1,2], Gang Cao[3], Jianshi Zhou[2], John B. Goodenough[2], Maxim Tsoi[1,2]

[1] *Physics Department, The University of Texas at Austin, Austin, Texas 78712, USA*

[2] *Texas Materials Institute, The University of Texas at Austin, Austin, Texas 78712, USA*

[3] *Department of Physics, University of Colorado-Boulder, Boulder, CO 80309, USA*

ABSTRACT

We study the resistive switching triggered by an applied electrical bias in antiferromagnetic Mott insulator $Sr_3Ir_2O_7$. The switching was previously associated with an electric-field driven structural transition. Here we use time-resolved measurements to probe the thermal activation behavior of the switching process and acquire information about the energy barrier associated with the transition. We quantify the changes in the energy barrier height with respect to the applied bias and find a linear decrease of the barrier with increasing bias. Our observations support the potential of antiferromagnetic transition metal oxides for spintronic applications.

Transition metal oxides (TMOs) exhibit a uniquely wide range of magnetic and transport properties with a tremendous potential for applications in various technologies [1]. For instance, the strong spin-orbit interaction in some TMOs can drive the J_{eff} =1/2 Mott state [2], superconductivity [3], topological insulator [4] and spin liquid [5] behaviors, which makes them an attractive playground for studying correlated electron physics. Applications of TMOs include, but are not limited to, spintronic [6] and resistive random access memory (ReRAM) devices [7, 8]. For example, antiferromagnetic (AFM) compounds are expected to improve stability, scalability, and speed of spintronic applications [9, 10], e.g. magnetic memories, thanks to the insensitivity of AFMs to magnetic fields and their high natural frequencies. Of particular interest are AFM TMOs as their properties can be tuned using various external stimuli, thus opening an entirely new dimension to the field of spintronics. Recently, we have demonstrated that the transport properties of AFM Mott insulators Sr_2IrO_4 and $Sr_3Ir_2O_7$ can be tuned by an externally applied electric field and found a reversible resistive switching driven by the electric bias [11, 12]. The switching was tentatively attributed to electric-field driven lattice distortions/structural transition with potential applications for writing in AFM and ReRAM memory applications.

In this Letter we probe the energy barrier associated with the switching transition in $Sr_3Ir_2O_7$. Time-resolved measurements were employed to probe the thermal activation behavior of the switching process and acquire information about the energy barrier associated with the transition. We observe an exponential dependence of the switching probability on both electric bias and temperature consistent with thermal activation over an energy barrier. We quantify the changes in the energy barrier height with respect to the applied bias and find a linear decrease of the barrier with increasing bias. Our observations elucidate the activation picture of resistive switching in Mott insulators and provide quantitative information about the switching barrier in $Sr_3Ir_2O_7$.

Single crystals of antiferromagnetic $Sr_3Ir_2O_7$ (T_N = 285 K) were synthesized for this work using a self-flux technique described elsewhere [13]. The technique results in single crystalline flakes of $Sr_3Ir_2O_7$ with thicknesses of about 0.2-mm and the [001] c-axis oriented perpendicular to the flake's surface (area ~0.5×0.5 mm^2). Single crystal X-ray diffraction was employed to determine the crystal structure of the flakes. Ag paste and In metal contacts (area ~0.2×0.2 mm^2) on top and bottom surfaces of $Sr_3Ir_2O_7$ flakes were used to supply and sink electrical currents (up to 15 mA). In

such a 2-probe geometry the applied currents flow (primarily) along the [001] c-axis of the crystal and were shown previously [14] to trigger a resistive switching at sufficiently high electrical bias. The switching was monitored by transport measurements – current-voltage (*I-V*) characteristics of the crystal were measured with the sample in liquid nitrogen (LN) in the temperature range from 77-80 K. The temperature control in this range was achieved by varying the LN pressure from 750-1020 Torr using an adjustable pressure relief valve on the LN cryostat. Time domain measurements were enabled by a Teledyne LeCroy Wavesurfer 3034 oscilloscope (350 MHz bandwidth, 4 GS/s) which was used to measure a delay time between the application of a bias current and the resistive switching. The delay time is projected to be conceptually similar to the decay time associated with the probabilistic processes governing radioactive decay.

Figure 1 shows a representative current-voltage (*I-V*) characteristic of $Sr_3Ir_2O_7$ measured at 77 K – the crystal resistance $R=V/I$ is shown as a function of the bias current I. Here the black and grey curves show the $R(I)$ for up- and down-sweeps of I, respectively. For an increasing bias, both positive and negative, we observe a continuous decrease of the crystal resistance and two irreversible switching events to a higher resistance (indicated by arrows in Fig. 1) at critical biases I_C ≈ ±8.5 mA and ±12.7 mA. For a decreasing bias, only one switching back to a lower resistance is observed at around ±5 mA. Similar switching characteristics were previously observed in both Sr_2IrO_4 and $Sr_3Ir_2O_7$ [12, 14] where the continuous/irreversible changes in resistance were associated with electric-field driven lattice distortions/structural transition. The inset to Fig. 1 shows the temperature dependence of the critical current associated with the lower-bias switching event at around 8.5 mA. Increasing the temperature of the sample has the effect of decreasing the critical bias current with a linear dependence quantified by 119 ± 3 μA/K.

Next we investigate the onset of the resistive switching in the time domain. We will focus on the lower-bias switching event around 8.5 mA (see Fig. 1). The procedure for triggering the switching consisted of slowly increasing the applied electrical bias from zero to a value (usually 8 mA) well below I_C and then abruptly (~150 μs) increasing the applied bias to a value above I_C. This abrupt jump in bias naturally produces an increase in the voltage across the crystal which has been used to trigger the oscilloscope. Figure 2 shows the resulting time evolution of voltage V_{OSC} across the sample measured by oscilloscope for a bias jump from 8 mA to 9.17 mA. Here the first rise in the oscilloscope voltage V_{OSC} at 0 ms is associated with the abrupt current jump from 8 to 9.17 mA;

the current jump produces the rise in V_{OSC} but the switching has not yet occurred. The switching is delayed and will happen a little later. We can clearly see a second rise in V_{OSC} at about 50 ms which is produced by an increase in the sample resistance (switching) which occurs with a delay $\tau \approx 50$ ms after the current jump. This increase in resistance corresponds to the increase in *R(I)* at 8.5 mA in Fig. 1. We thus conclude that the resistive switching requires a certain time τ at a given bias (I = 9.17 mA). We have repeated the above measurement 600 times and found a distribution of delay times shown in the inset to Fig. 2. The associated Poisson fit (solid curve in the inset) suggests that on average the switching at I = 9.17 mA is delayed by about 50 ms.

We can use the measured delay time to determine the activation energy of switching. A simple model where the switching is associated with overcoming an energy barrier Δ implies the Arrhenius equation for the delay time:

$$\tau = \tau_0 \, e^{\frac{\Delta}{k_B T}} \qquad [1]$$

with τ_0 the attempt time (reciprocal of the attempt frequency), k_B Boltzmann constant, and T temperature. Assuming τ_0 = 1 ns and using T = 77 K in our experiment, this analysis yields Δ = 50 meV. While the exact value of τ_0 in our system is unknown, this analysis provides a reasonable estimation of Δ, since decreasing τ_0 by as much as three orders of magnitude (to 1 ps) would increase Δ by only 20 meV. In contrast, the variation of the energy barrier Δ with respect to the applied bias current I can be characterized exactly as we show next.

The procedure for finding the average delay time at a given switching current I was repeated for different Is. These measurements have provided the $\tau(I)$ dependence displayed in Fig.3. Here open symbols show that the delay time increases significantly with decreasing bias current I. By applying Eq. 1 to every τ data point in Fig. 3 we have reconstructed the dependence of Δ on I. The inset to Fig. 3 shows that the energy barrier Δ decreases approximately linearly with the applied bias current I (see the linear fit in Fig.3 inset). This result correlates with the field-effect model, which was used to explain the linear relationship between the activation energy and applied electrical bias observed in $Sr_3Ir_2O_7$ [14]. In this model an applied electric field alters the equilibrium positions of oxygen with respect to iridium ions and induces distortions of the corner shared IrO_6 octahedra, thus, provoking modifications of the localized states and electronic structure [12, 14]. These (reversible) distortions are responsible for the continuous decrease in resistance with increasing bias observed in

Fig. 1. The switching in this model is tentatively associated with a bias-induced structural transition between two metastable states separated by an energy barrier. The field-effect model suggests that the switching barrier in Eq. 1 can be expressed as a function of the applied bias as:

$$\Delta = \Delta_0 - \gamma I \qquad [2]$$

where Δ_0 is the barrier at zero I and γ is the parameter which characterizes the strength of the field effect. From the linear data fit in Fig. 3 inset we now define the γ parameter – 172 eV/A. Using this parameter we have successfully fitted the $\tau(I)$ data in Fig. 3 (see solid curve) by an exponential function which combines Eqs. 1 and 2:

$$\tau = \tau_0\, e^{\frac{\Delta_0 - \gamma I}{k_B T}} \qquad [3]$$

Note that the effect of Joule heating can be ruled out as a possible source of Δ-variations in our experiment. In Fig. 3 we observe a strong variation of the delay time τ as a function of the bias current – the delay time changes by a factor of ≈50. If triggered by temperature alone, the 50-fold decrease of τ requires an increase in temperature by about 50% (Eq. 1). The actual increase of the bias current (<0.8% in Fig. 3) increases the Joule heating power by less than 0.64% and can only increase the sample temperature by less than ~1%. We thus conclude that Joule heating cannot explain our observations in Fig. 3; it is due to the effect of electric bias on τ.

We have also verified experimentally that the resistive switching (Fig. 1) and its thermal-activation behavior (Figs. 2 and 3) are not affected by an externally applied magnetic field up to 0.25 T (maximum field available in our experiments). This result is in agreement with previous observations of zero magnetotransport response in $Sr_3Ir_2O_7$ [14].

Now we can verify Eq. 3 by performing our experiment at different temperatures. In our set-up the sample is immersed in liquid nitrogen to maximize the heat removal and minimize any Joule heating from high bias currents. The sample temperature can be accurately controlled in the range from 77-80 K by controlling the pressure (from 750-1020 Torr) in the nitrogen cryostat using an adjustable pressure relief valve. Note that the pressure of the nitrogen column above the sample should also be taken into account in order to determine the actual temperature of the sample using the well-established temperature/pressure relation for liquid nitrogen [15].

Figure 4a shows the average switching delay vs applied bias (as in Fig. 3) measured at eleven different temperatures in the range from 77-80 K. Equation 3 was successfully used to fit the data at different temperatures (see solid curves); the curves shift to the left with increasing temperature. Using Eq. 1 we have reconstructed *Δ(I)* for different temperatures which are shown in Fig. 4b with the corresponding linear fits. Using the fits for Δ, we can define an effective current, I_{eff}, that represents the temperature variation of an average delay time associated with a particular value of Δ. Figure 4c shows $I_{eff}(T)$ for $\Delta = 60$ meV. The temperature dependent variation of I_{eff} is analogous to the previous temperature-dependent measurement of the critical switching current I_C. Indeed, the slope of $I_{eff}(T)$ – 110 ± 1 μA/K, is comparable to the slope of $I_C(T)$ – 119 ± 3 μA/K. We should note that our method to control the temperature may cause some of the observed effects to be associated with the pressure variations. It is possible that the changes we observed in transport properties of our samples are caused directly by the pressure. However, given a very large magnitude of pressure (on the order of GPa) needed to induce transport effects in iridates [16-19], we estimate the effects from pressure on the order of an atmosphere to be negligible. Therefore we attribute the observed in Fig.4 changes in Δ to the effect of temperature on Δ_0 while the bias-dependent component of Δ characterized by γ varies very little in the above temperature range (77-80 K).

In summary, we have investigated the energy landscape of bias induced resistive switching in antiferromagnetic $Sr_3Ir_2O_7$. Using temporally resolved transport measurements, a bias and temperature dependent switching delay time was observed. A model based on thermally assisted transitions over an energy barrier was used to explain the observed behavior. The energy barrier's dependence on applied bias and temperature was quantified. An electric field effect model describing induced structural modifications can be used to explain both discontinuous changes in $Sr_3Ir_2O_7$ resistance and well as previously demonstrated electrically tunable transport in $Sr_3Ir_2O_7$ and Sr_2IrO_4 [12, 20]. These findings are of high interest for future antiferromagnetic spintronics and spin dynamics with the general goal of high-speed applications controlled by electric fields.

This work was supported in part by C-SPIN, one of six centers of STARnet, a Semiconductor Research Corporation program, sponsored by MARCO and DARPA, by NSF grants DMR-1712101 and DMR-1122603, and by the King Abdullah University of Science and Technology (KAUST) Office of Sponsored Research (OSR) under Award No. OSR-2015-CRG4-2626.

References:

[1] P. A. Cox, *Transition Metal Oxides* (Oxford University Press, 2010).

[2] B. J. Kim, Hosub Jin, S. J. Moon, J.-Y. Kim, B.-G. Park, C. S. Leem, Jaejun Yu, T. W. Noh, C. Kim, S.-J. Oh, J.-H. Park, V. Durairaj, G. Cao, and E. Rotenberg, Phys. Rev. Lett. 101, 076402 (2008).

[3] F. Wang, T. Senthil, Phys. Rev. Lett. 106, 136402 (2011).

[4] D. Pesin, L. Balents, Nature Physics 6, 376 (2010).

[5] Y. Okamoto, M. Nohara, H. Aruga-Katori, and H. Takagi, Phys. Rev. Lett. 99, 137207 (2007).

[6] M. Bibes, A. Barthélémy, IEEE Trans. Electron Devices 54, 1003 (2007).

[7] H. Akinaga, H. Shima, Proc. IEEE 98, 2237 (2010).

[8] H.-S. P. Wong, H.-Y. Lee, S. Yu, Y.-S. Chen, Y. Wu, P.-S. Chen, B. Lee, F. T. Chen, and M.-J. Tsai, Proc. IEEE 100, 1951 (2012).

[9] A. H. MacDonald, M. Tsoi, Phil. Trans. R. Soc. A 369, 3098 (2011).

[10] V. Baltz, A. Manchon, M. Tsoi, T. Moriyama, T. Ono, and Y. Tserkovnyak, Rev. Mod. Phys. 90, 015005 (2018).

[11] C. Wang, H. Seinige, G. Cao, J.-S. Zhou, J. B. Goodenough, and M. Tsoi, Phys. Rev. X **4**, 041034 (2014).

[12] C. Wang, H. Seinige, G. Cao, J.-S. Zhou, J. B. Goodenough, and M. Tsoi, Phys. Rev. B **92**, 115136 (2015).

[13] G. Cao, Y. Xin, C. S. Alexander, J. E. Crow, P. Schlottmann, M. K. Crawford, R. L. Harlow, and W. Marshall, Phys. Rev. B **66**, 214412 (2002).

[14] H. Seinige, M. Williamson, S. Shen, C. Wang, G. Cao, J.-S. Zhou, J. B. Goodenough, and M. Tsoi, Phys. Rev. B 94, 214434 (2016).

[15] J. E. Jensen, W. A. Tuttle, R. B. Stewart, H. Brechna, and A. G. Prodell, *Brookhaven National Laboratories Selected Cryogenic Data Notebook* (BNL, New York, 1980)

[16] D. Haskel, G. Fabbris, M. Zhernenkov, P. P. Kong, C. Q. Jin, G. Cao, and M. van Veenendaal, Phys. Rev. Lett. **109**, 027204 (2012)

[17] Y. Ding, L. Yang, C.-C. Chen, H.-S. Kim, M. J. Han, W. Luo, Z. Feng, M. Upton, D. Casa, J. Kim, T. Gog, Z. Zeng, G. Cao, H. Mao, and M. van Veenendaal, Phys. Rev. Lett. **116**, 216402 (2016)

[18] D. A. Zocco, J. J. Hamlin, B. D. White, B. J. Kim, J. R. Jeffries, S. T. Weir, Y. K. Vohra, J. W. Allen, and M. B. Maple, J. Phys. Condens. Matter **26**, 255603 (2014).

[19] C. Donnerer, Z. Feng, J. G. Vale, S. N. Andreev, I. V. Solovyev, E. C. Hunter, M. Hanfland, R. S. Perry, H. M. Rønnow, M. I. McMahon, V. V. Mazurenko, and D. F. McMorrow, Phys. Rev. B **93**, 174118 (2016).

[20] C. Hahn, G. de Loubens, V. V. Naletov, J. B. Youssef, O. Klein and M. Viret, Europhys. Lett. **108**, 57005 (2014).

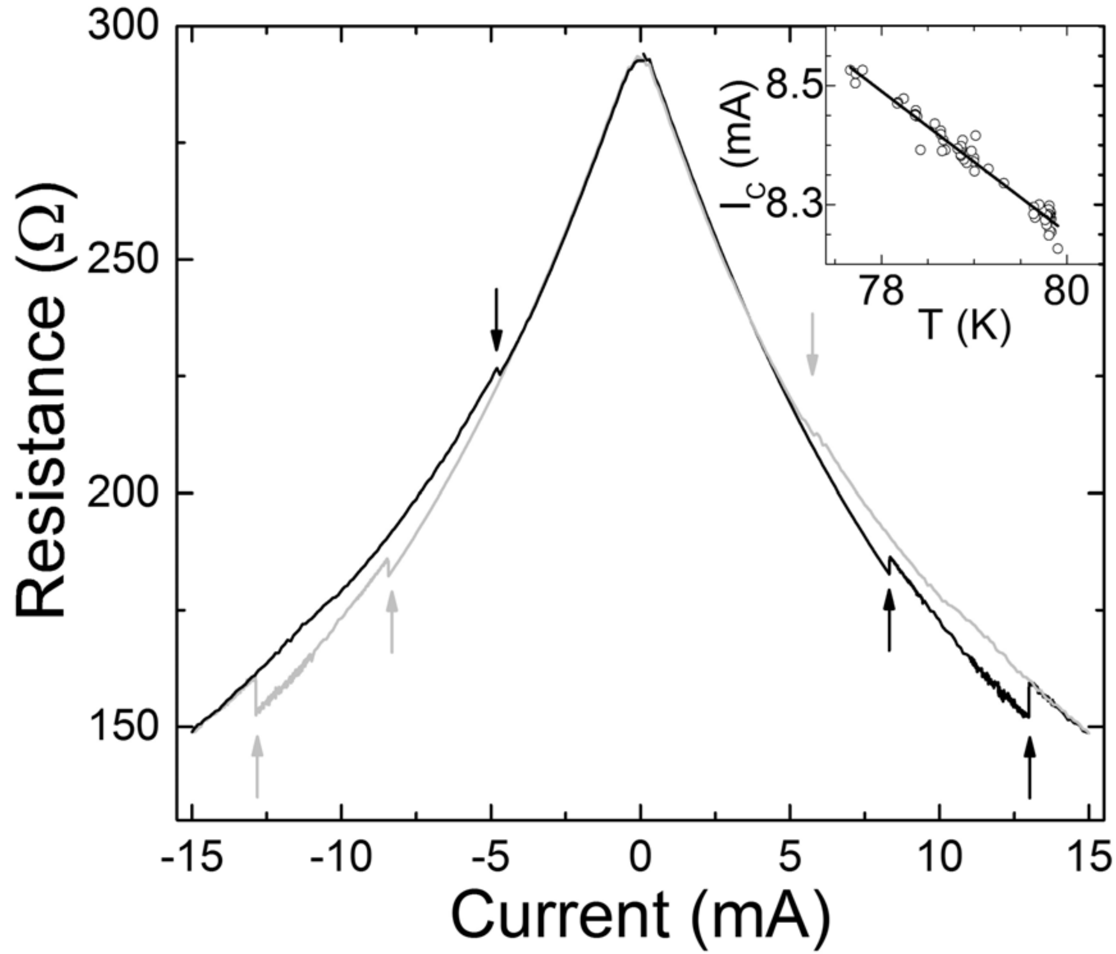

Figure 1: (a) Resistive switching in $R(I)$ characteristic of $Sr_3Ir_2O_7$ (T = 78.6 K). Black (gray) trace represents the I-sweep from -15 mA to +15 mA (from +15 mA to -15 mA). Arrows indicate switching events. Two switching events to a higher resistance for increasing bias (at I_c=±8.5 mA and ±12.7 mA) and one to a lower resistance for decreasing bias are clearly visible. The inset shows the temperature dependence of the critical current associated with the first switching event at I_c=8.5 mA.

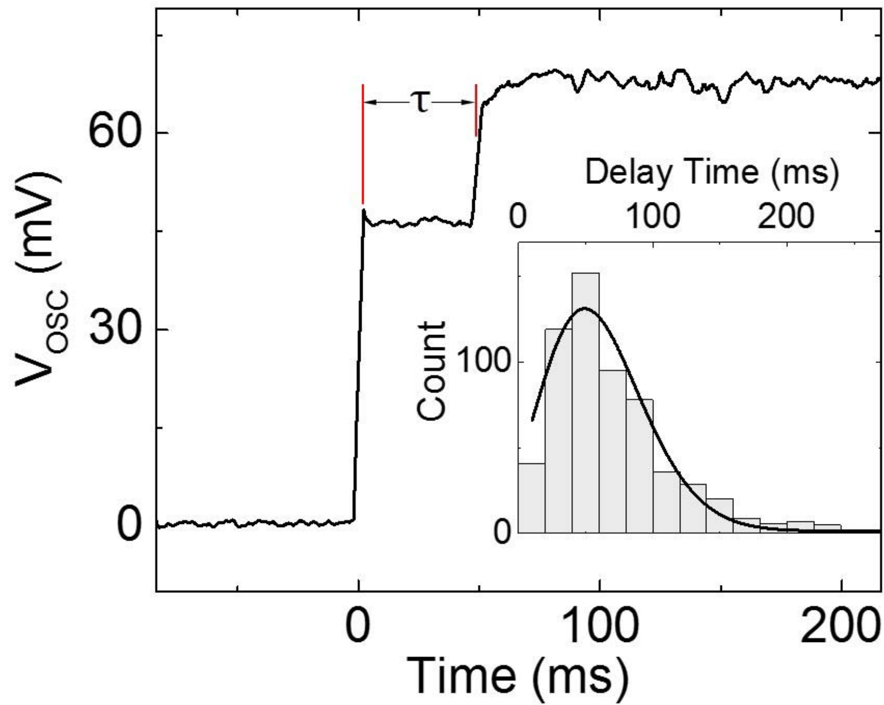

Figure 2: (a) A time trace of the process of switching from low bias to the '1st high-resistance' state. The vertical axis plots the voltage across the sample captured with an oscilloscope where the first abrupt increase is caused by a sudden rise in applied current. After a time, τ, the switching occurs resulting in a second abrupt rise in measured voltage due to an increase in sample resistance indicating that switching has occurred. Figure 2b shows the results of the mentioned measurement repeated 600 times. A histogram corresponding to the relative frequency of measured delay time values is plotted with a Poisson fit.

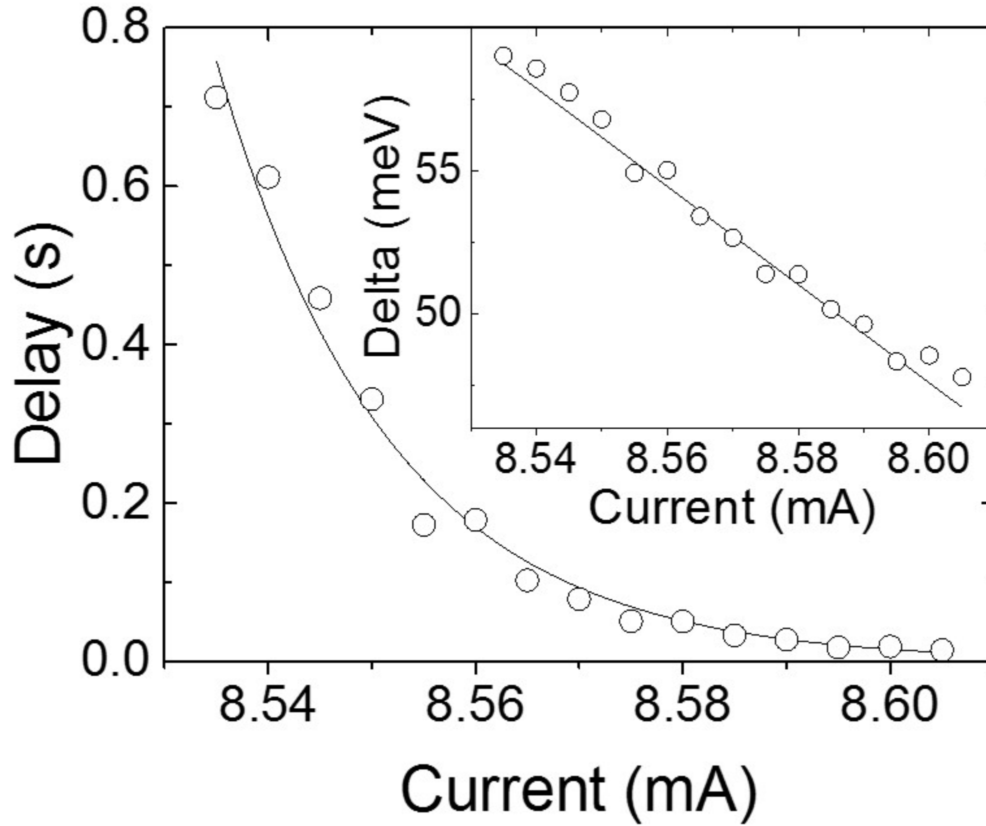

Figure 3: (a) Average delay time between application of current step and resistive switching as a function of the final bias measured at 77 K. All switching events were executed from a beginning bias of 8.0 mA. Solid line shows exponential fit. The inset depicts the change in the barrier height, Δ, as a function of the final bias with a linear fit corresponding to a modulation of 172 meV/mA.

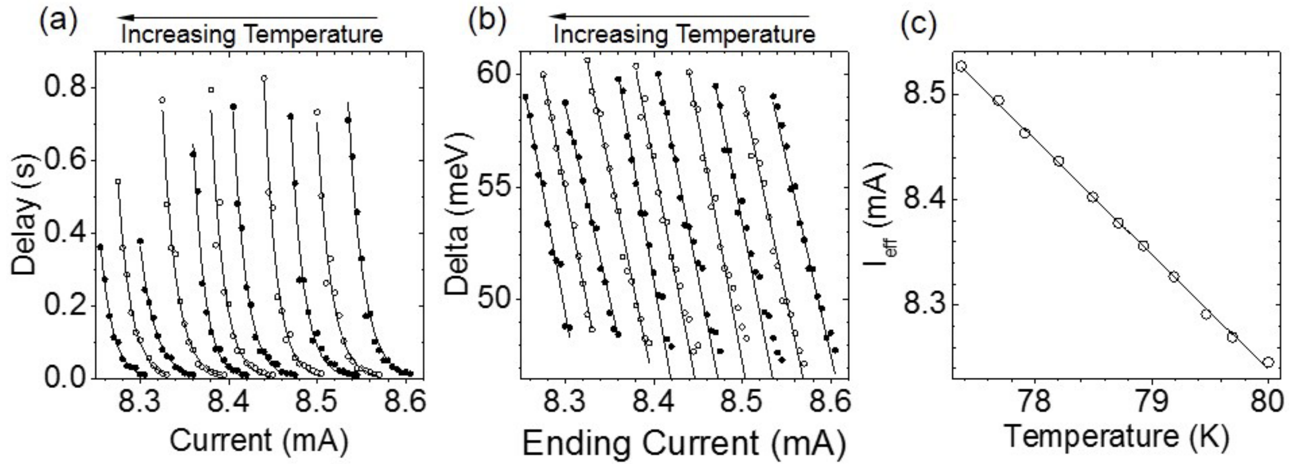

Figure 4: (a) Temperature effects of the average delay measurement shown in figure 3. Temperatures range from 77 K at the rightmost curve to 80 K at the leftmost curve. Black and white symbols serve to separate data associated with neighboring temperatures. (b) Delta calculated as a function of temperature (τ_0 = 1 ns). (c) The change in the current, I_{eff} associated with delta equal to 60 meV, as a function of temperature with a linear fit corresponding to a variation of 110 ± 1 μA/K.